Striatal GABAergic and cortical glutamatergic neurons mediate contrasting effects of cannabinoids on cortical network synchrony

Carola Sales-Carbonell[a,b,c,d], Pavel E. Rueda-Orozco[a,b,c,d], Edgar Soria-Gómez[e,f], György Buzsáki[g], Giovanni Marsicano[e,f], and David Robbe[a,b,c,d,1]

[a]Department of Systems Neuroscience, Institut d'Investigacions Biomèdiques August Pi i Sunyer, 08016 Barcelona, Spain; [b]Institut National de la Santé et de la Recherche Médicale (INSERM) U901, 13273 Marseille, France; [c]Aix-Marseille University, Unité Mixte de Recherche 901, 13273 Marseille, France; [d]Institut de Neurobiologie de la Méditerranée, 13273 Marseille, France; [e]INSERM U862, Neurocentre Magendie, 33077 Bordeaux, France; [f]Université de Bordeaux 2, 33077 Bordeaux, France; and [g]Neuroscience Institute, New York University School of Medicine, New York, NY 10016

Edited by Leslie Lars Iversen, University of Oxford, Oxford, United Kingdom, and approved November 30, 2012 (received for review October 2, 2012)

Activation of type 1 cannabinoid receptors (CB1R) decreases GABA and glutamate release in cortical and subcortical regions, with complex outcomes on cortical network activity. To date there have been few attempts to disentangle the region- and cell-specific mechanisms underlying the effects of cannabinoids on cortical network activity in vivo. Here we addressed this issue by combining in vivo electrophysiological recordings with local and systemic pharmacological manipulations in conditional mutant mice lacking CB1R expression in different neuronal populations. First we report that cannabinoids induce hypersynchronous thalamocortical oscillations while decreasing the amplitude of faster cortical oscillations. Then we demonstrate that CB1R at striatonigral synapses (basal ganglia direct pathway) mediate the thalamocortical hypersynchrony, whereas activation of CB1R expressed in cortical glutamatergic neurons decreases cortical synchrony. Finally we show that activation of CB1 expressed in cortical glutamatergic neurons limits the cannabinoid-induced thalamocortical hypersynchrony. By reporting that CB1R activations in cortical and subcortical regions have contrasting effects on cortical synchrony, our study bridges the gap between cellular and in vivo network effects of cannabinoids. Incidentally, the thalamocortical hypersynchrony we report suggests a potential mechanism to explain the sensory "high" experienced during recreational consumption of marijuana.

cannabis | high-voltage spindles | striatum | substantia nigra | electrocorticograms

Cannabinoids are a family of compounds that activate cannabinoid receptors, which are well known for their psychotropic effects and therapeutic potentials. The type 1 cannabinoid receptor (CB1R) is massively expressed in the brain at the synaptic terminals of excitatory and inhibitory neurons, and its activation by exogenous or endogenous cannabinoids decreases neurotransmitter release (1–3). One largely unanswered question is how the elementary decreases in excitatory and inhibitory synaptic transmissions induced by systemic intake of cannabinoids interact to produce alterations in neuronal network activity in vivo. A number of recent studies combining systemic injections of CB1R agonists and antagonists with electrophysiological recordings in the hippocampus and neocortex of awake or anesthetized rodents have shown that a hallmark of cannabinoids effects on neuronal network activity is a decrease in synchrony (4–9). Specifically, systemic CB1R activation has been shown to decrease (*i*) the amplitude of the hippocampal θ rhythm (4, 7, 8), (*ii*) the amplitude of γ oscillations in the hippocampus (4, 7, 10), enthorinal cortex (8), and prefrontal cortex (7), (*iii*) the incidence of hippocampal ripples (4, 6, 11), and (*iv*) spiking correlation in the hippocampus and prefrontal cortex (4, 5, 7, 9).

In contrast to the consistent reports that cannabinoids dampen cortical network oscillations, other findings suggest that they could also increase synchrony. First, CB1R are predominantly expressed by GABAergic forebrain neurons (12), and their activation leads to decreased GABA release (1). Therefore, cannabinoids might be expected to increase network synchrony or generate excessive firing activity, in a similar manner to GABA receptors antagonists, which favor convulsive seizures (13, 14). Second, several studies have reported that cannabinoids are proconvulsant in experimental models of epilepsy (15–17). The concurrent but unbalanced activation of the CB1R at the synaptic terminals of inhibitory and excitatory neurons could be one explanation for these seemingly contradictory observations. Additionally, the high level of CB1R expression in subcortical regions (18–20) leaves open the possibility that at least a part of the cannabinoid-induced alterations in cortical network activity has extracortical origins. To date, the potential cell type- and region-specific impact of CB1R activation on in vivo cortical network activity has received little attention. Here we specifically addressed this issue by comparing the impact of systemic and local injections of the CB1R agonist CP55940 on cortical network oscillations recorded from freely moving mice lacking CB1R expression in distinct neuronal populations. The results reveal the cell- and region-specific mechanisms underlying a dual modulation of cortical synchrony by exogenous cannabinoids and pave the way to a refined understanding of the cognitive alterations associated with marijuana consumption (21, 22).

Results

Systemic CB1R Activation Induces Thalamocortical High-Voltage Spindles While Decreasing Fast Electrocorticogram Oscillations. To investigate in vivo the cell type-specific impact of systemic CB1R activation on cortical network activity, we recorded neocortical electrocorticograms (ECoG) before and after i.p. injections of the high-affinity CB1R agonist CP55940 (0.3 mg/kg of body weight). ECoG were recorded bilaterally above the somatosensory cortex, in the home cage of two groups of mice: C57BL/6N mice ($n = 9$) and conditional mutant mice that lack CB1R expression in specific neuronal populations [$n = 33$, including WT littermates (19, 23, 24)]. All ECoG shown and compared in this study were taken from periods of immobility, to avoid biased quantification of network activity due to decreased locomotor activity induced by the systemic injection of cannabinoids (19) (Fig. S1). We first examined and quantified the impact of CP55940 on the oscillatory content of

Author contributions: G.B., G.M., and D.R. designed research; C.S.-C., P.E.R.-O., E.S.-G., and D.R. performed research; G.M. contributed new reagents/analytic tools; C.S.-C. and D.R. analyzed data; and G.B., G.M., and D.R. wrote the paper.

The authors declare no conflict of interest.

This article is a PNAS Direct Submission.

[1]To whom correspondence should be addressed. E-mail: david.robbe@inserm.fr.

This article contains supporting information online at www.pnas.org/lookup/suppl/doi:10.1073/pnas.1217144110/-/DCSupplemental.

the ECoG from C57BL/6N mice (Fig. 1). After CP55940 injections the ECoG displayed numerous oscillatory bursts, with a shape, frequency (~5 Hz), length (~1–2 s), and amplitude (> 0.5 mV) characteristic of thalamocortical high-voltage spindles (HVS, also referred to as spike-and-wave discharges/seizures) (Fig. 1 *A*–*C*; arrowheads in Fig. 1*C*) (25–27). As expected for this type of oscillation, HVS were sparse during control recordings (27) and, after CP55940 injections, were strictly restricted to periods of immobility (28). A quantitative routine developed to compare HVS before and after CP55940 injections (*Experimental Procedures*, Fig.

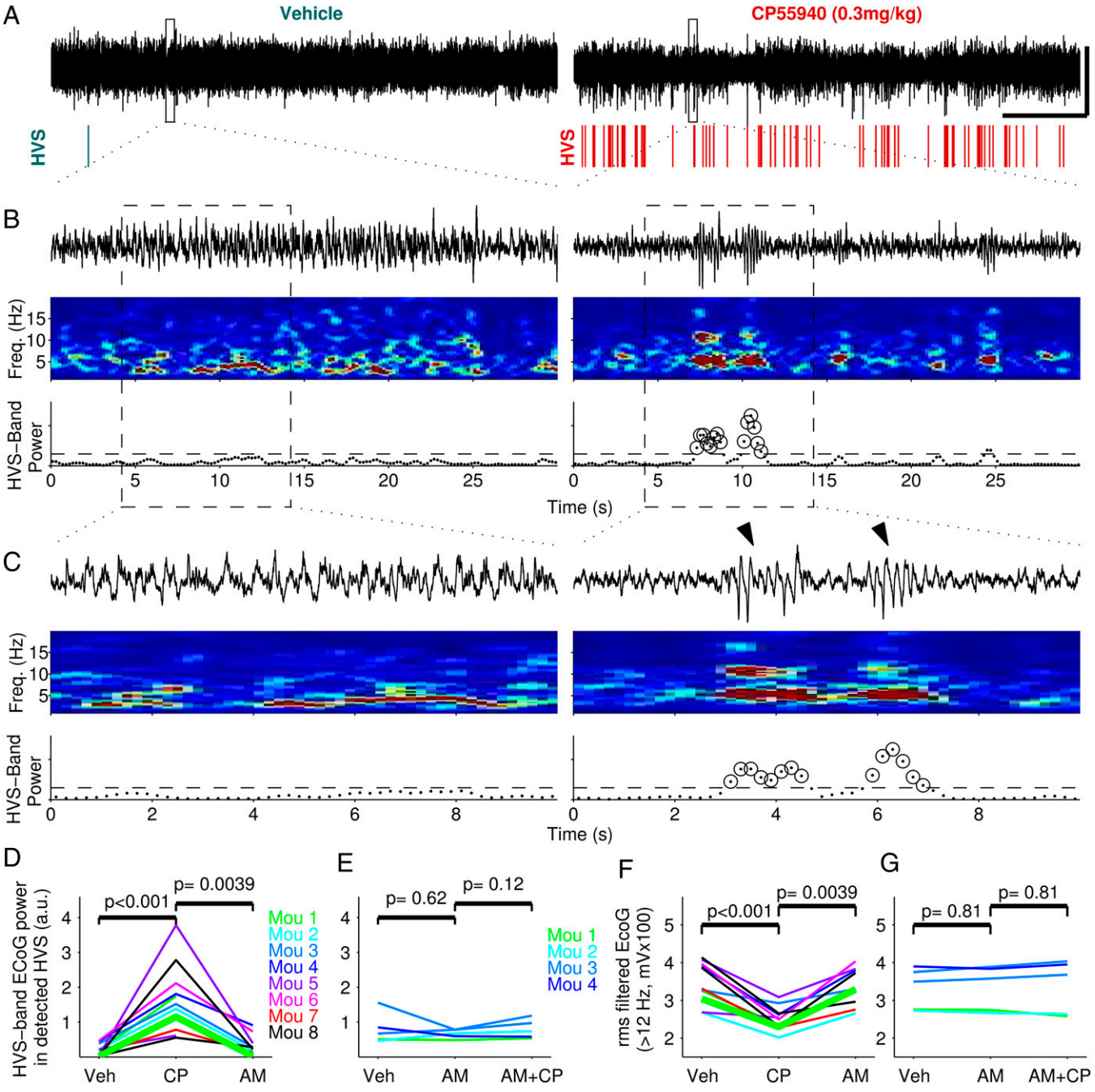

Fig. 1. Systemic CB1R activation induces HVS while decreasing the amplitude of faster neocortical oscillations. (*A*–*C*) Single experiment showing the effects of an i.p. injection of the CB1R agonist CP55940 (*Right*), or its vehicle alone (*Left*), on a mouse ECoG recorded during immobility epochs. (*A*) Thirty minutes ECoG (black traces) and HVS incidence (colored rasters). (Scale bars, 1 mV and 5 min.) (*B*) Thirty seconds ECoG taken from rectangles in *A*. (*Middle*) Time–frequency power spectrograms (1-s sliding windows, steps of 0.2 s). (*Bottom*) ECoG power values in the HVS frequency band (4–6 Hz). Dashed line is HVS detection threshold. Circles identify windows detected as part of an HVS. (*C*) Similar to *B*, but 10 s ECoG are from dashed rectangles in *B*. Arrowheads indicate detected HVS. ECoG traces in *A*–*C* have the same voltage scale. (*D* and *E*) HVS comparison in all experiments. Each line represents a single experiment, and different colors represent different animals. CP55940 (CP, 0.3 mg/kg) reliably increases HVS, and this effect was reversed (*D*) and abolished (*E*) by injection of the CB1R antagonist AM251 (AM, 3 mg/kg). (*F* and *G*) Similar to *D* and *E*, but the amplitude of ECoG oscillations faster than 12 Hz is compared. Same experiments and color code as in *D* and *E*. *P* values in *D*–*G* are from Wilcoxon paired two-sided signed rank test. Bold green traces in *D* and *F* show the quantification of the illustrative experiment shown in *A*–*C*.

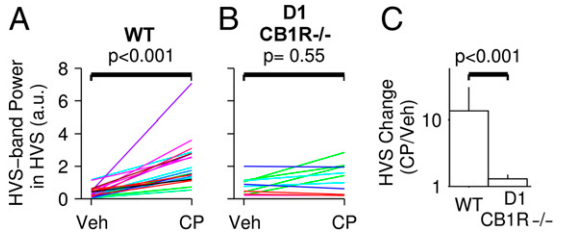

Fig. 2. CB1R expressed by D1-positive striatal neurons are required for the CP55940-induced increase in HVS. (*A* and *B*) Group effect of vehicle and CP55940 (CP, 0.3 mg/kg) injections on HVS in WT animals (*A*) and mice lacking CB1R expression in D1-positive striatal neurons (D1-CB1R$^{-/-}$; *B*). (*C*) Comparison of the effects of CP55940 on HVS between WT and D1-CB1R$^{-/-}$ mice. Histograms show mean changes in HVS power and incidence. Error bars are SEM. *P* value is from the Wilcoxon rank sum test.

1 *B* and *C*, and Fig. S2) showed that, across animals and experiments, HVS incidence and power reliably and strongly increased after CP55940 injections (Fig. 1*D*). This effect was dependent on CB1R activation because it was completely reversed (Fig. 1*D* and Fig. S3) and prevented (Fig. 1*E*) by i.p. injections of the CB1R antagonist AM251 (3 mg/kg). Cannabinoids have been previously shown to decrease the power of neocortical local field potential oscillations over a wide range of frequencies (7, 8). Therefore, we next quantified the effect of CP55940 on ECoG oscillations in a frequency band distinct from the one of the cannabinoid-induced HVS. As expected, CP55940 injections reliably decreased the amplitude of fast (>12 Hz) ECoG oscillations (Fig. 1*F*) (7, 8), an effect that was also reversed (Fig. 1*F* and Fig. S3) and blocked (Fig. 1*G*) by AM251 injections. Taken together these data show that systemic CB1R activation, although decreasing synchrony of fast ECoG oscillations, generated hypersynchronous oscillatory bursts characteristic of thalamocortical HVS.

CB1R Activation at GABAergic Striatonigral Synapses Increases the Incidence of Thalamocortical HVS. We next set out to understand how CP55940 i.p. injections increase HVS. Although rodent HVS function is still a matter of debate [analog to human μ rhythm (29) or model for absence-like seizure actvity (30)], there is ample evidence that they share mechanistic similarities with the well-studied thalamocortical sleep spindle oscillations (31–35). On the one hand, the basal ganglia is a major site controlling thalamocortical oscillations (28, 36) via giant inhibitory nigrothalamic synapses (37). Specifically, potentiation or blockade of GABAergic transmission in the substantia nigra pars reticulata (SNr) decreases or increases HVS incidence, respectively (36, 38). On the other hand, the highest density of CB1R in the brain is found in the SNr on striatal inhibitory terminals (1, 20), where CB1R activation potently decreases GABA release (39). To test the hypothesis that CB1R expressed by striatonigral neurons (D1-positive medium spiny neurons forming the basal ganglia direct pathway) mediate the increase in HVS observed after systemic injection of CP55940, we took advantage of conditional mutant mice lacking CB1R expression in the striatal neurons projecting to the SNr (D1-CB1R$^{-/-}$ mice) (19). In WT mice, CP55940 systemic injections induced HVS (Fig. 2*A*), but no such effect was seen in the D1-CB1R$^{-/-}$ mice (Fig. 2 *B* and *C*). CP55940 effects on HVS were also abolished in GABA-CB1R$^{-/-}$ and CaMK-CB1R$^{-/-}$ mice (Fig. S4), which lack CB1R expression in, respectively, GABAergic and principal forebrain neurons (24). In GABA-CB1R$^{-/-}$ and CaMK-CB1R$^{-/-}$ mice, striatal neurons projecting to the SNr lack CB1R expression. Thus, this result (Fig. S4) confirms that CB1R expressed by striatonigral neurons is required for the CP55940-induced increase in HVS. Importantly, the ECoG oscillatory content during baseline recordings was similar across all types of conditional mutant mice (Fig. S5), ruling out the possibility that the differential effects of CP55940 in WT and CB1R mutant mice originate from alterations in baseline cortical network activity.

The lack of cannabinoid-induced enhancement in HVS in D1-CB1R$^{-/-}$ mice suggested that, in the SNr, activation of CB1R expressed by striatonigral neurons is necessary to increase HVS. To test more directly this hypothesis, CP55940 was locally injected in the SNr of WT and D1-CB1R$^{-/-}$ mice. In WT mice, injections of CP55940 in the SNr induced HVS, an effect that could be reversed by a subsequent injection of the GABA-A receptor agonist muscimol (Fig. 3 *A* and *B*). Conversely, in D1-CB1R$^{-/-}$ mice, intra-SNr injections of CP55940 failed to increase HVS (Fig. 3 *C* and *D*; $P < 0.001$ vs. WT data), whereas subsequent injections of the GABA-A antagonist bicuculline increased HVS (Fig. 3*C*). Altogether these results are consistent with a scenario in which CP55940 enhances HVS incidence by decreasing GABA release from direct pathway striatal neurons projecting to the SNr.

Activation of CB1R Expressed by Cortical Glutamatergic Neurons Decreases Fast Neocortical Oscillations and Limits Cannabinoid-Induced Increase in HVS. Systemic injection of CP55940 enhances HVS while decreasing the power of fast (>12 Hz) ECoG oscillations in mice

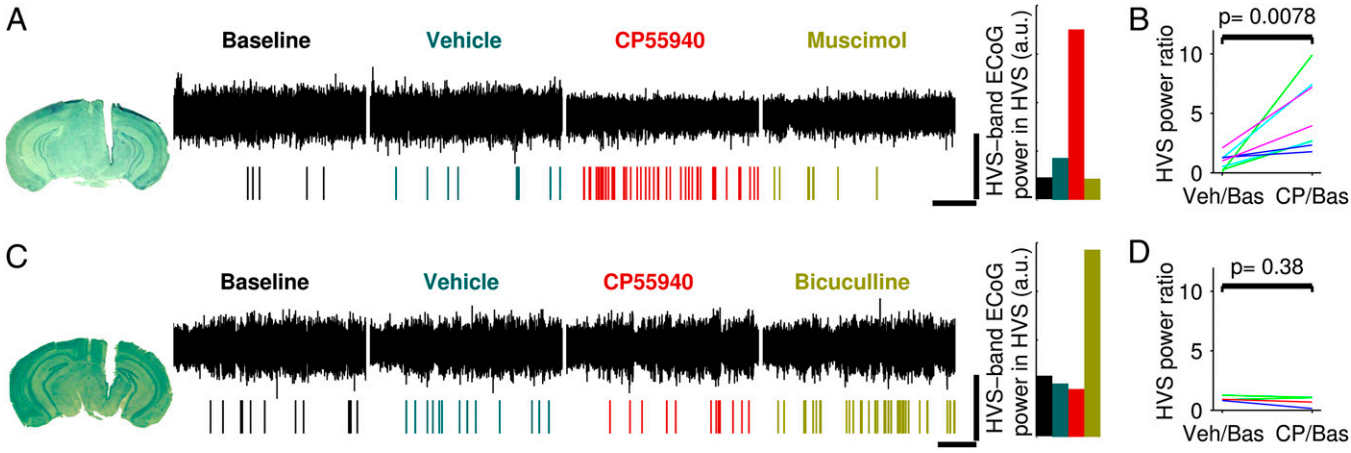

Fig. 3. Intra-SNr activation of CB1R expressed by D1-positive striatal neurons induces HVS. (*A* and *C*) Single experiments in WT (*A*) and D1-CB1R$^{-/-}$ (*C*) mice. (*Left*) Track of the injection cannula. Black traces are ECoG during baseline and after injections (500 nL) of vehicle, CP55940 (20 mg/mL), and muscimol (0.5 mg/mL; *A*) or bicuculline (0.2 mg/mL; *C*). Rasters show detected HVS. Colored histograms show HVS power and incidence quantification for these two experiments. (*B* and *D*) Group effect of intra-SNr CP55940 (CP) injections on HVS in WT (*B*) and D1-CB1R$^{-/-}$ (*D*) mice. (Scale bars, 5 min and 1 mV.)

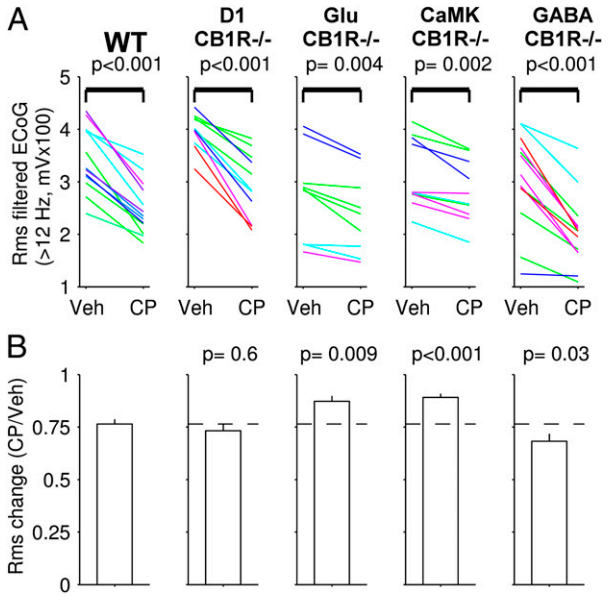

Fig. 4. Cannabinoid-induced decrease in fast ECoG oscillations power is reduced in mice lacking CB1R in glutamatergic cortical neurons. (*A*) Effects of vehicle and CP55940 (CP) injections on the amplitude of fast (>12 Hz) ECoG oscillations in, from left to right, WT, D1-CB1R$^{-/-}$ mice, mice lacking CB1R in glutamatergic cortical neurons (Glu-CB1R$^{-/-}$), in all principal forebrain neurons (CaMK-CB1R$^{-/-}$), and in all GABAergic forebrain neurons (GABA-CB1R$^{-/-}$). (*B*) Mean changes in HVS and SEM for WT and mutant mice. *P* values are from Wilcoxon rank sum test vs. WT data. Dotted lines represent mean change in the WT group.

(Fig. 1). To test whether these effects shared the same mechanism, we quantified the effect of CP55940 on the amplitude of fast ECoG oscillations in CB1R conditional mutant mice and their WT littermates. The CP55940-induced decrease in fast ECoG oscillations power was intact in D1-CB1R$^{-/-}$ mice (Fig. 4), suggesting that the cannabinoid-induced increase in HVS and decrease in fast ECoG oscillations have distinct mechanisms. In contrast, the decrease in fast ECoG oscillations was significantly reduced in Glu-CB1R$^{-/-}$ and CaMK-CB1R$^{-/-}$ mice compared with WT littermates (Fig. 4). These results show that activation of CB1R expressed by glutamatergic cortical neurons is, at least in part, responsible for the reduced neuronal network synchrony observed in vivo after cannabinoids injections. Additionally, CP55940-induced decrease in fast ECoG oscillations was stronger in GABA-CB1R$^{-/-}$ mice than in WT littermates (Fig. 4), suggesting that activations of CB1R expressed on cortical GABAergic and glutamatergic neurons exert a bidirectional control over fast ECoG oscillations.

A desynchronization function of CB1R expressed by glutamatergic cortical neurons is additionally supported by the observation that the cannabinoid-induced increase in HVS was stronger in Glu-CB1R$^{-/-}$ mice than in WT animals (Fig. 5 *A*–*C*). Indeed, CP55940 induced prominent HVS and high-amplitude isolated spike-and-wave complexes in the mutant mice (Fig. 5 *D* and *E*). This result suggests that, in WT animals, activation of CB1R expressed by glutamatergic cortical neurons limits the increase in HVS observed after CP55940 injection.

Discussion

Here we report that cannabinoids have contrasting effects on neocortical network synchrony, characterized by the appearance of hypersynchronous thalamocortical oscillations and decreased amplitude of fast ECoG oscillations. Taking advantage of conditional mice lacking CB1R expression in specific neuronal populations, we broke down these effects into region- and cell-specific CB1R activation: CB1R at striatonigral inhibitory synapses are responsible for the cannabinoid-induced thalamocortical hypersynchrony, whereas CB1R activation at cortical excitatory synapses reduces synchrony of fast neocortical oscillations.

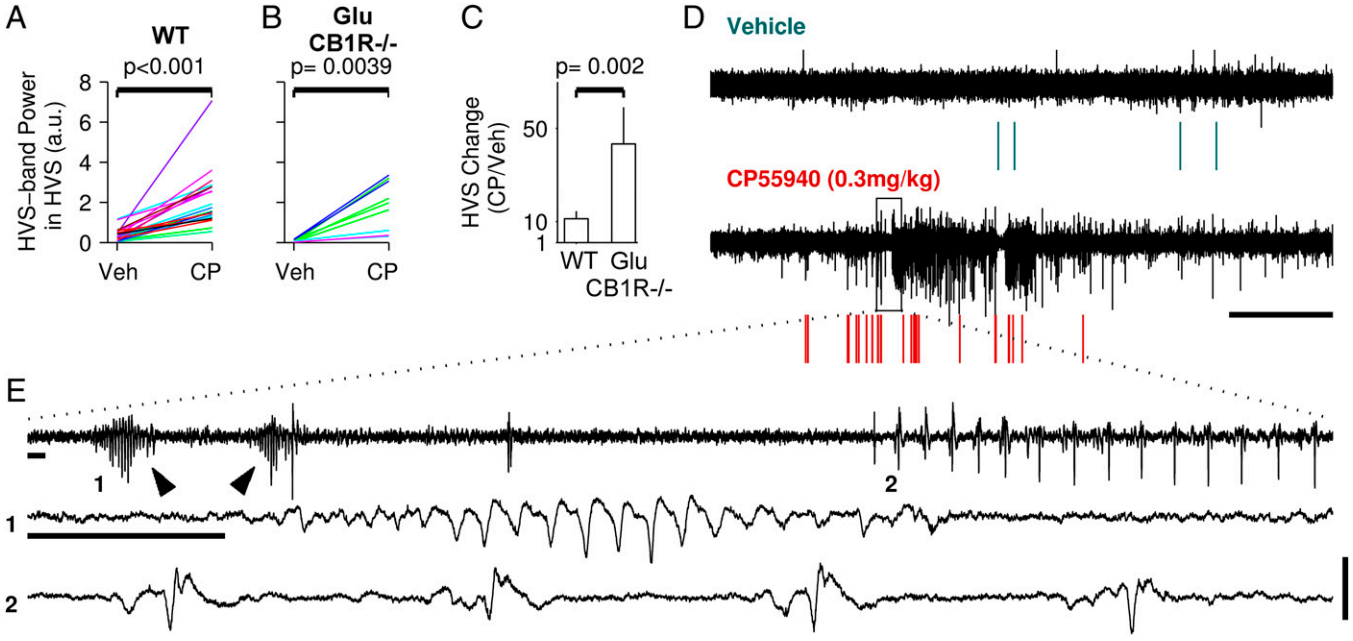

Fig. 5. CB1R expressed by glutamatergic cortical neurons limit the cannabinoid-induced increase in HVS. (*A* and *B*) Effects of vehicle and CP55940 (CP) injections on HVS incidence and power in WT (*A*) and Glu-CB1R$^{-/-}$ (*B*) mice. (*C*) Comparison of the mean changes in HVS for these mice. (*D*) Single experiment in which ECoG (black) was recorded from a Glu-CB1R$^{-/-}$ mouse after vehicle (*Upper*) and CP55940 (*Lower*) i.p. injections. Colored rasters show detected HVS. (Scale bar, 5 min.) (*E*) Upper trace is taken from the rectangle in *D*. Arrowheads show two HVS. The two lower traces are taken from the upper trace (1, 2) and show, respectively, a strong HVS and isolated spike-and-wave seizure-like discharges. (Scale bars, 1 s and 0.75 mV.)

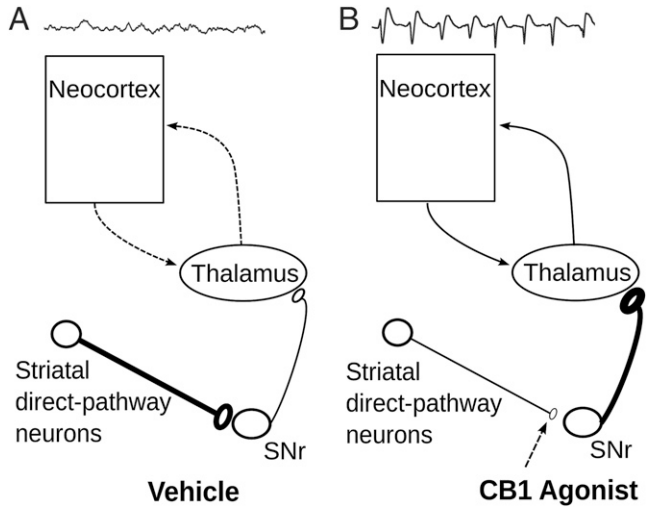

Fig. 6. Hypothesized mechanism responsible for the cannabinoid-induced thalamocortical HVS. (*A* and *B*) Schematic representation of the circuit responsible for HVS control during vehicle (*A*) or CB1R agonist (*B*) injections. During vehicle injection the oscillation-promoting nigrothalamic GABAergic neurons are kept inhibited by striatonigral inhibitory neurons. After cannabinoid injection, the nigrothalamic oscillation-promoting neurons are disinhibited after CB1R activation at striatonigral synapses.

We found that in immobile mice, systemic CB1R activation generated highly synchronous oscillatory bursts of the ECoG with a frequency, duration, and amplitude characteristic of thalamocortical HVS (25, 26, 40). We further showed that this hypersynchronous effect was mediated by CB1R located in the SNr on striatal GABAergic synaptic terminals. Finally, intra-SNr injections of GABA-A agonist and antagonist, respectively, reversed and mimicked the effects of CP55940 on HVS. Altogether, our results are best explained by the following mechanism: systemic CB1R activation induces thalamocortical HVS by decreasing GABA release at striatonigral synapses (Fig. 6). This hypothesis is supported by previous studies on CB1R synaptic physiology in the basal ganglia and the known role of the SNr in controlling thalamocortical oscillations. First, the highest level of CB1R immunoreactivity in rodent is found in the SNr (18). In this nucleus, CB1R is localized on axons and terminals of striatal neurons (20), and its activation potently inhibits striatonigral GABAergic transmission (20, 39). Second, the basal ganglia are known to modulate thalamocortical oscillations (28, 36). Specifically, hyperpolarization of thalamocortical relay cells is a condition sine qua non for the emergence of thalamocortical oscillations (13, 31, 34), and the giant inhibitory synapses between GABAergic neurons of the SNr and thalamocortical relay cells have been proposed to contribute to this hyperpolarization (37). In agreement with an oscillation-promoting role of nigrothalamic cells, pharmacological excitation or inhibition of SNr neurons increased or decreased HVS incidence, respectively (38, 41). Finally, dopamine depletion or blockade of dopamine receptors in the striatum, which decreased the activity of direct pathway striatal neurons (42), also enhanced the incidence of HVS (28, 43). Altogether these studies suggest that the cannabinoid-induced increase in HVS we report is best explained by the disinhibition of nigrothalamic GABAergic neurons (Fig. 6).

In mice lacking CB1R on glutamatergic cortical neurons (Glu-CB1R$^{-/-}$), the cannabinoid-induced increase in HVS was stronger than in their WT littermates, and CP55940 generated a seizure-like pattern of activity. This result suggests that in WT mice, striatonigral and cortical CB1R compete and modulate thalamocortical oscillations in opposite directions. The partial counterbalancing effect of "cortical" CB1R could be due to a decrease in release of glutamate in the neocortex, in the thalamus (from corticothalamic excitatory neurons), or in both areas. This is in agreement with a role of cortical input on the thalamic reticular neurons to control thalamocortical HVS oscillations (34, 44). A role for CB1R expressed by cortical glutamatergic neurons in reducing network synchrony is further supported by the observation that cannabinoid-induced decrease in fast neocortical oscillations was reduced in Glu- and CaMK-CB1R$^{-/-}$ mice. This function is in line with studies showing that "glutamatergic cortical" CB1R provide protection against kainic acid-induced seizures (23, 24) and with recent works suggesting that cannabinoids decrease hippocampal γ and ripple oscillations by decreasing excitatory transmission (6, 11). CB1R expressed by brain astroglial cells have been recently shown to participate in the control of glutamatergic synaptic transmission and plasticity (45–47). Our results suggest that the effects of CP55940 on fast ECoG oscillations are mostly independent from astroglial CB1R: in fact, at odds with astroglial CB1R-dependent long-term depression of excitatory synaptic transmission (47), CP55940 effects were reversed by injections of a CB1R antagonist and were significantly reduced in Glu-CB1R$^{-/-}$ mice. Still, at this stage, we cannot entirely exclude that astroglial CB1R contribute to the decrease in fast ECoG oscillations, and future investigation will address directly this possibility.

There are several possible specific behavioral implications of our findings. First, the reported dual pro- and antioscillatory functions of CB1R expressed in, respectively, subcortical and cortical regions might be related to the complex control of network excitability exerted by CB1R in physiopathological conditions, such as during epileptiform seizures (15–17, 23, 48). Additionally, we believe that the increase in thalamocortical HVS after CB1R activation in the SNr offers a perspective to understand the psychoactive effects associated with marijuana consumption. In this context, it is important to emphasize that thalamocortical HVS have been proposed to constitute a brain state that facilitates detection of weak sensory stimulation (29, 49). More generally, the activity of the thalamocortical system controls vigilance states and gates the perception of sensory stimulation (50). The recreational consumption of marijuana is well known to produce a "high" characterized by an altered consciousness and an intensification of sensory perceptions (51). Strikingly, in both human and rodent brains, the highest expression of CB1R is found in the SNr on striatonigral synapses (18, 20, 52, 53). Therefore, an exciting hypothesis for future investigation is that the sensory/behavioral "high" experienced during marijuana consumption is due to an aberrant thalamocortical synchrony via massive CB1R activation in the SNr.

Experimental Procedures

Experimental procedures are described in *SI Experimental Procedures*. This section describes the conditional CB1R mutant mice used, electrophysiological recording methods, local and systemic pharmacological injections, and data analysis. All animal procedures were conducted in accordance with standard ethical guidelines (European Communities Directive 86/60-EEC) and were approved by the local ethical committee (Comité d'Experimentació Animal, Universitat de Barcelona, Ref 520/08).

ACKNOWLEDGMENTS. We thank O. Manzoni, I. Bureau, H. Martin, and D. Jercog for excellent discussions and careful reading of the manuscript; D. Gonzales, N. Aubailly, M. Metna, D. Terrier, and T. Wiesner for mouse care and genotyping; and A. Cei for help in early experiments on this project. This work was funded by Ministerio de Ciencia e Innovación Grant BFU2008-03946 (to D.R.), Marie Curie International Reintegration Grant IRG230976 (to D.R.), Institut National de la Santé et de la Recherche Médicale (INSERM) (G.M.), Region Aquitaine (E.S.-G. and G.M.), and the European Research Council (ERC-2010-StG-260515, to G.M.). D.R. was supported by a Ramon-Y-Cajal fellowship from the Spanish Ministerio de Ciencia e Innovación and the Avenir program from INSERM. P.E.R.-O. was supported by Marie Curie International Incoming Fellowship IIF253873. E.S.-G. was supported by the Fyssen Fondation.

1. Freund TF, Katona I, Piomelli D (2003) Role of endogenous cannabinoids in synaptic signaling. *Physiol Rev* 83(3):1017–1066.
2. Piomelli D (2003) The molecular logic of endocannabinoid signalling. *Nat Rev Neurosci* 4(11):873–884.
3. Kano M, Ohno-Shosaku T, Hashimotodani Y, Uchigashima M, Watanabe M (2009) Endocannabinoid-mediated control of synaptic transmission. *Physiol Rev* 89(1): 309–380.
4. Robbe D, et al. (2006) Cannabinoids reveal importance of spike timing coordination in hippocampal function. *Nat Neurosci* 9(12):1526–1533.
5. Robbe D, Buzsáki G (2009) Alteration of theta timescale dynamics of hippocampal place cells by a cannabinoid is associated with memory impairment. *J Neurosci* 29(40): 12597–12605.
6. Maier N, et al. (2012) Cannabinoids disrupt hippocampal sharp wave-ripples via inhibition of glutamate release. *Hippocampus* 22(6):1350–1362.
7. Kucewicz MT, Tricklebank MD, Bogacz R, Jones MW (2011) Dysfunctional prefrontal cortical network activity and interactions following cannabinoid receptor activation. *J Neurosci* 31(43):15560–15568.
8. Hajós M, Hoffmann WE, Kocsis B (2008) Activation of cannabinoid-1 receptors disrupts sensory gating and neuronal oscillation: Relevance to schizophrenia. *Biol Psychiatry* 63(11):1075–1083.
9. Goonawardena AV, Riedel G, Hampson RE (2011) Cannabinoids alter spontaneous firing, bursting, and cell synchrony of hippocampal principal cells. *Hippocampus* 21(5): 520–531.
10. Hájos N, et al. (2000) Cannabinoids inhibit hippocampal GABAergic transmission and network oscillations. *Eur J Neurosci* 12(9):3239–3249.
11. Holderith N, et al. (2011) Cannabinoids attenuate hippocampal γ oscillations by suppressing excitatory synaptic input onto CA3 pyramidal neurons and fast spiking basket cells. *J Physiol* 589(Pt 20):4921–4934.
12. Marsicano G, Kuner R (2008) *Cannabinoids and the Brain*, ed Köfalvi A (Springer, New York), pp 161–201.
13. Steriade M, Contreras D (1998) Spike-wave complexes and fast components of cortically generated seizures. I. Role of neocortex and thalamus. *J Neurophysiol* 80(3): 1439–1455.
14. Vergnes M, Boehrer A, Simler S, Bernasconi R, Marescaux C (1997) Opposite effects of GABAB receptor antagonists on absences and convulsive seizures. *Eur J Pharmacol* 332(3):245–255.
15. Turkanis SA, Karler R (1982) Central excitatory properties of delta 9-tetrahydrocannabinol and its metabolites in iron-induced epileptic rats. *Neuropharmacology* 21(1): 7–13.
16. Fish BS, Consroe P, Fox RR (1983) Convulsant-anticonvulsant properties of delta-9-tetrahydrocannabinol in rabbits. *Behav Genet* 13(2):205–211.
17. Clement AB, Hawkins EG, Lichtman AH, Cravatt BF (2003) Increased seizure susceptibility and proconvulsant activity of anandamide in mice lacking fatty acid amide hydrolase. *J Neurosci* 23(9):3916–3923.
18. Herkenham M, et al. (1990) Cannabinoid receptor localization in brain. *Proc Natl Acad Sci USA* 87(5):1932–1936.
19. Monory K, et al. (2007) Genetic dissection of behavioural and autonomic effects of Delta(9)-tetrahydrocannabinol in mice. *PLoS Biol* 5(10):e269.
20. Mátyás F, et al. (2006) Subcellular localization of type 1 cannabinoid receptors in the rat basal ganglia. *Neuroscience* 137(1):337–361.
21. Meier MH, et al. (2012) Persistent cannabis users show neuropsychological decline from childhood to midlife. *Proc Natl Acad Sci USA* 109(40):E2657–E2664.
22. Bossong MG, et al. (2012) Effects of δ9-tetrahydrocannabinol on human working memory function. *Biol Psychiatry* 71(8):693–699.
23. Marsicano G, et al. (2003) CB1 cannabinoid receptors and on-demand defense against excitotoxicity. *Science* 302(5642):84–88.
24. Monory K, et al. (2006) The endocannabinoid system controls key epileptogenic circuits in the hippocampus. *Neuron* 51(4):455–466.
25. Arain FM, Boyd KL, Gallagher MJ (2012) Decreased viability and absence-like epilepsy in mice lacking or deficient in the GABAA receptor α1 subunit. *Epilepsia* 53(8): e161–e165.
26. Ernst WL, Zhang Y, Yoo JW, Ernst SJ, Noebels JL (2009) Genetic enhancement of thalamocortical network activity by elevating alpha 1g-mediated low-voltage-activated calcium current induces pure absence epilepsy. *J Neurosci* 29(6):1615–1625.
27. Ryan LJ (1984) Characterization of cortical spindles in DBA/2 and C57BL/6 inbred mice. *Brain Res Bull* 13(4):549–558.
28. Buzsáki G, Smith A, Berger S, Fisher LJ, Gage FH (1990) Petit mal epilepsy and parkinsonian tremor: Hypothesis of a common pacemaker. *Neuroscience* 36(1):1–14.
29. Wiest MC, Nicolelis MA (2003) Behavioral detection of tactile stimuli during 7-12 Hz cortical oscillations in awake rats. *Nat Neurosci* 6(9):913–914.
30. Shaw F-Z (2004) Is spontaneous high-voltage rhythmic spike discharge in Long Evans rats an absence-like seizure activity? *J Neurophysiol* 91(1):63–77.
31. Beenhakker MP, Huguenard JR (2009) Neurons that fire together also conspire together: Is normal sleep circuitry hijacked to generate epilepsy? *Neuron* 62(5):612–632.
32. Kandel A, Buzsáki G (1997) Cellular-synaptic generation of sleep spindles, spike-and-wave discharges, and evoked thalamocortical responses in the neocortex of the rat. *J Neurosci* 17(17):6783–6797.
33. McCormick DA, Bal T (1997) Sleep and arousal: Thalamocortical mechanisms. *Annu Rev Neurosci* 20:185–215.
34. Timofeev I, Steriade M (2004) Neocortical seizures: Initiation, development and cessation. *Neuroscience* 123(2):299–336.
35. Buzsáki G (1991) The thalamic clock: Emergent network properties. *Neuroscience* 41(2-3):351–364.
36. Deransart C, Vercueil L, Marescaux C, Depaulis A (1998) The role of basal ganglia in the control of generalized absence seizures. *Epilepsy Res* 32(1-2):213–223.
37. Bodor AL, Giber K, Rovó Z, Ulbert I, Acsády L (2008) Structural correlates of efficient GABAergic transmission in the basal ganglia-thalamus pathway. *J Neurosci* 28(12): 3090–3102.
38. Deransart C, Lê-Pham BT, Hirsch E, Marescaux C, Depaulis A (2001) Inhibition of the substantia nigra suppresses absences and clonic seizures in audiogenic rats, but not tonic seizures: Evidence for seizure specificity of the nigral control. *Neuroscience* 105(1):203–211.
39. Wallmichrath I, Szabo B (2002) Cannabinoids inhibit striatonigral GABAergic neurotransmission in the mouse. *Neuroscience* 113(3):671–682.
40. Radek RJ, Curzon P, Decker MW (1994) Characterization of high voltage spindles and spatial memory in young, mature and aged rats. *Brain Res Bull* 33(2):183–188.
41. Paz JT, Chavez M, Saillet S, Deniau JM, Charpier S (2007) Activity of ventral medial thalamic neurons during absence seizures and modulation of cortical paroxysms by the nigrothalamic pathway. *J Neurosci* 27(4):929–941.
42. Mallet N, Ballion B, Le Moine C, Gonon F (2006) Cortical inputs and GABA interneurons imbalance projection neurons in the striatum of parkinsonian rats. *J Neurosci* 26(14):3875–3884.
43. Dejean C, Gross CE, Bioulac B, Boraud T (2008) Dynamic changes in the cortex-basal ganglia network after dopamine depletion in the rat. *J Neurophysiol* 100(1):385–396.
44. Polack P-O, Mahon S, Chavez M, Charpier S (2009) Inactivation of the somatosensory cortex prevents paroxysmal oscillations in cortical and related thalamic neurons in a genetic model of absence epilepsy. *Cereb Cortex* 19(9):2078–2091.
45. Navarrete M, Araque A (2010) Endocannabinoids potentiate synaptic transmission through stimulation of astrocytes. *Neuron* 68(1):113–126.
46. Min R, Nevian T (2012) Astrocyte signaling controls spike timing-dependent depression at neocortical synapses. *Nat Neurosci* 15(5):746–753.
47. Han J, et al. (2012) Acute cannabinoids impair working memory through astroglial CB1 receptor modulation of hippocampal LTD. *Cell* 148(5):1039–1050.
48. Lutz B (2004) On-demand activation of the endocannabinoid system in the control of neuronal excitability and epileptiform seizures. *Biochem Pharmacol* 68(9):1691–1698.
49. Nicolelis MAL, Fanselow EE (2002) Thalamocortical optimization of tactile processing according to behavioral state. *Nat Neurosci* 5:517–523.
50. Steriade M (2000) Corticothalamic resonance, states of vigilance and mentation. *Neuroscience* 101(2):243–276.
51. Iversen L (2000) *The Science of Marijuana* (Oxford Univ Press, New York).
52. Mailleux P, Vanderhaeghen JJ (1992) Localization of cannabinoid receptor in the human developing and adult basal ganglia. Higher levels in the striatonigral neurons. *Neurosci Lett* 148(1-2):173–176.
53. Glass M, Dragunow M, Faull RL (1997) Cannabinoid receptors in the human brain: A detailed anatomical and quantitative autoradiographic study in the fetal, neonatal and adult human brain. *Neuroscience* 77(2):299–318.

Supporting Information

Sales-Carbonell et al. 10.1073/pnas.1217144110

SI Experimental Procedures

All animal procedures were conducted in accordance with standard ethical guidelines (European Communities Directive 86/60-EEC) and were approved by the local ethics committee (Comité d'Experimentació Animal, Universitat de Barcelona, Ref 520/08).

Animals. In vivo chronic electrocorticogram (ECoG) recordings were performed in three groups of animals: (*i*) 9 C57BL/6N (Charles River), (*ii*) conditional type 1 cannabinoid receptor (CB1R) mutant mice (4 Glu-CB1R$^{-/-}$, 5 GABA-CB1R$^{-/-}$, 4 CaMK-CB1R$^{-/-}$, and 7 D1-CB1R$^{-/-}$), and (*iii*) 13 WT littermates (1–3). All mice (male and female) were aged 4–7 mo. Regarding ECoG baseline activity and CP55940 effects on ECoG, no differences between sexes were observed. Similarly, no differences were observed between WT littermates of the four different mutant lines. Therefore, all WT animals were pooled into a single group for statistical comparison. Glu-CB1R$^{-/-}$ mice lack CB1R expression in dorsal telencephalon glutamatergic neurons, including neurons located in neocortex, paleocortex, archicortex, hippocampal formation, and cortical portions of the amygdala; GABA-CB1R$^{-/-}$ mice lack CB1R expression mainly from forebrain GABAergic neurons; CaMK-CB1R$^{-/-}$ mice lack CB1R expression in all forebrain principal neurons; and D1-CB1R$^{-/-}$ mice lack CB1R expression in cells expressing D1-type dopamine receptors, including striatal medium spiny neurons (1, 2, 4). Conditional CB1R mutant mice were generated in a predominant C57BL/6N background (back-crossed for at least five generations) and were genotyped before and after the experiments, as previously described (2). A few days before surgical implantations of chronic recording electrodes, animals were housed individually in the experimental laboratory in stable conditions of temperature (22 °C) and humidity (60%), with a constant cycle of 12 h light and 12 h dark and ad libitum access to food and water. Animals were given at least 1 wk of recovery time after the surgery before recordings started.

Surgical Procedures. All surgical procedures were performed with stereotaxic control under deep isoflurane anesthesia. In the majority of chronic recordings performed in mice, miniature stainless steel screws (Small Parts, size 000-120) were implanted epidurally above the somatosensory cortex [anteroposterior (AP): −0.5 mm; mediolateral (ML): ±3 mm, relative to Bregma). In a few mice, recordings were additionally performed above the prefrontal cortex (AP: +1.5; ML: ±0.75) and/or in the CA1 hippocampus pyramidal layer. Two miniatures screws implanted above cerebellum served as ground and reference.

For local injection experiments, mice were additionally implanted with a single stainless steel guide cannula (26 gauge; PlasticsOne) aimed at the dorsal border of the substantia nigra pars reticulata (AP: −3.4 mm; ML: ±1.37 mm; dorsoventral: −2.75 mm). The tip injector protruded 1 mm below the tip of the guide cannula.

Drugs Preparations. For i.p. injections, CP55940 and AM251 (Vitro) were dissolved in a 1:1:18 vehicle solution of DMSO (Sigma): cremophor-EL (Sigma):saline. The volume of the injections was 10 mL/kg of body weight. The dosage for CP55940 and AM251 i.p. injections was 0.3 and 3 mg/kg of body weight, respectively. For local injection experiments, 10 μg of CP55940, dissolved in 0.5 μL of vehicle (same as above), were injected. A muscimol (Tocris) solution (0.5 μL of 0.5 mg/mL in saline) and 0.5 μL of a (-)-bicuculline methiodide (Tocris) solution (0.2 mg/mL in saline) were also injected in WT and D1-CB1R$^{-/-}$ mice, respectively.

Chronic in Vivo Recordings and Local Injection Procedures. Wideband (0.1 Hz–8 kHz) neurophysiological signals (amplified 1,000 times via a Plexon HST/16V-G20 headstage and a Plexon PBX2 amplifier) and acceleration signals (1–50 Hz) were digitized at 1 kHz on two synchronized National Instruments A/D cards (PCI 6254, 16-bit resolution).

Locomotor activity was quantified either with two silver bipolar electromyography (EMG) electrodes inserted in the dorsal nuchal (neck) muscles or with a triple-axis miniature accelerometer affixed to the recording headstage (ADXL 335, SparkFun Electronics) (5). In this last case, the signal of the accelerometer *z* axis (vertical) was used.

Control recordings started 15 min after connection of the animal to the amplifier or vehicle i.p. injections. "Drug" recordings started 15 min after i.p. injections. Three types of experiments were performed: (*i*) vehicle-CP55940, (*ii*) vehicle-CP55940-AM251, and (*iii*) vehicle-AM251-[CP55940+AM251]. In the case of type-2 experiments, at least 2 h 30 min-long recordings were performed after AM251 injection to allow for complete reversion of the CP55940 effect. The ECoGs analyzed were then taken starting 1 h 30 min after AM251 i.p. injection. The rationale for this is the well-known slow reversibility of CB1R agonist effects by CB1R antagonist, which is explained by the lipophilic nature of CP55940 and AM251 and the better CB1R affinity of the former vs. the latter compound. One to three experiments were performed in each animal, depending on the quality of the electrophysiological signal. Experiments performed in the same animal were interleaved with at least 5 d without any injection.

For local injection procedures in awake mice, animals were manually restrained from the recording headstage, the dummy cannula was gently removed, and the injector was slowly inserted through the guide cannula. The injector was connected via a polyethylene tube (PE50; Plastics One) to a Hamilton microsyringe driven by a microinfusion pump (11 plus; Harvard Apparatus). A volume of 500 nL was injected at a rate of 200 nL/min. To allow complete diffusion of the drug, the injector was left in place 2 min after injection before being removed and replaced by the dummy. After baseline recording, the injection order was vehicle-CP55940-muscimol (or bicuculline in CB1R-D1$^{-/-}$ mice). Electrophysiological recordings consisted of at least 20 min of immobility epochs in each condition, starting just after local injections.

At the end of the experiments, mice were deeply anesthetized and their brain fixed with an intracardiac perfusion of 10% formalin solution. The brains were sliced (50 μm), and Nissl staining was performed to confirm the position of injection cannulae.

Behavioral Activity Quantification. Neck EMG or head acceleration signals were respectively high-pass filtered above 40 Hz and band-pass filtered between 2 and 20 Hz. The filtered signals were squared and smoothed with an averaged filter of 500 ms. The resulting signal provided a time-varying estimate of behavioral activity. Because the quality of EMG recording and the exact position of the accelerometer vary across days and between animals, the threshold value to separate immobility from mobility was adjusted manually. To this end, the time-varying behavioral estimate was overlaid with the simultaneously recorded ECoG. ECoG oscillatory content depends on behavioral activity, and this property was used to adjust precisely the threshold. The same threshold was used for control and drug recordings to be compared. If the interval between two consecutive mobility periods was less than 4 s, these periods were merged.

Power Spectrum Analysis. Spectral analyzes were made using a multitaper approach as implemented in the Chronux toolbox (http://chronux.org/). ECoG was digitally high-pass filtered at 1 Hz. Frequency-domain analysis was restricted to data recorded during immobility periods. Power spectrum density functions were computed with nine tapers and averaged over 10-s–long epochs.

High-Voltage Spindles Comparison. Comparison of high-voltage spindles (HVS) incidence and power between control and drug conditions was made from ECoG (25–30 min long) recorded during periods of immobility (i.e., periods of immobility, interleaved by behavioral activity, were concatenated until they amounted to 25–30 min). The rationale for comparing HVS over such relatively short periods was to avoid as much as possible the inclusion of slow-wave sleep in our control recordings. During immobility, the incidence of HVS in mice was extremely low in control condition but strongly and reliably increased after CP55940 systemic injection (6). Noticeably, across experiments and animals, we found variability in the mean frequency of the HVS appearing after CP55940 injections (range, 4–8 Hz). The first step of our HVS quantification consisted therefore in determining the cannabinoid-induced HVS frequency band. To avoid ECoG power at low frequencies (<3 Hz) contaminating the estimation of the HVS frequency band (owing to the presence 1/f pink noise in this type of signal), the ECoG obtained after CP55940 injection was detrended (locdetrend function in Chronux toolbox, 300-ms–long moving windows). The average power spectrum density function of the detrended ECoG was computed as described earlier. The HVS frequency band was defined as a 2-Hz–wide window centered around the peak of the power spectrum in the drug condition (Fig. S2*A*, *1*). Using a distinct method (7) to reduce 1/f pink noise in the ECoG resulted in similar results. Note that ECoG detrending was only done to define the HVS frequency band. CP55940 globally reduced the amplitude of the ECoG fluctuations (Fig. 1). To avoid this effect affecting HVS detection, the ECoGs to compare were standardized. Time–frequency spectrograms of the standardized ECoGs were computed (1-s–long windows, advanced in steps of 0.2 s; examples in Fig. 1*C* and Fig. S2*B*). For each window, the power in the HVS frequency band was calculated (Fig. S2 *A*, *2*). An arbitrary threshold for HVS detection was then defined as the mean plus 2 SDs of the HVS frequency band power values obtained in all of the windows (vehicle + CP55940, Fig. S2 *A*, *3*). HVS were defined as the times when four or more consecutive windows had power values in the HVS frequency band superior to the threshold (Fig. 1 *B* and *C* and Fig. S2 *A*, *4* and *B*). Finally, the time–frequency spectrograms of the ECoGs (nonstandardized) were computed as above. In the pharmacological conditions to compare (e.g., vehicle vs. CP55940), we computed the sum of the ECoG power in the HVS frequency band from the windows detected as part of an HVS (Fig. S2 *A*, *5*). These sums provide a quantification of HVS incidence and power during a single experiment. It is very important to note that the threshold is a relative value that depends on the intraexperiment variability of the ECoG power in the HVS frequency band. For instance, a strong increase in HVS after CP55940 injection would bias the threshold toward a high value. Consequently, the number of detected HVS after vehicle injection would be low. Conversely, if a CP55940 injection had little effect on HVS (as in the D1-CB1R$^{-/-}$ mice), the threshold would be low and more HVS would be detected in the control recording (this is the reason why baseline HVS incidence is higher in Fig. 3*C* than in Fig. 3*A*). Using this "relative" method to compare HVS in a given pharmacological condition (e.g., vehicle) between different animals or experiments is therefore meaningless. Only change in HVS power and incidence (calculated as the ratio "HVS in CP55940"/"HVS in vehicle") were compared across animals.

Statistics. To statistically assess electrophysiological differences between pharmacological conditions (e.g., vehicle vs. CP55940) in a given group of animals (e.g., WT mice) we used the Wilcoxon paired signed rank test (nonparametric test). To statistically assess differences in CP55940 effect between two groups of animals (e.g., WT vs. Glu-CB1R$^{-/-}$ mice) we used the Wilcoxon rank sum test (nonparametric test).

1. Monory K, et al. (2007) Genetic dissection of behavioural and autonomic effects of Delta(9)-tetrahydrocannabinol in mice. *PLoS Biol* 5(10):e269.
2. Monory K, et al. (2006) The endocannabinoid system controls key epileptogenic circuits in the hippocampus. *Neuron* 51(4):455–466.
3. Marsicano G, et al. (2003) CB1 cannabinoid receptors and on-demand defense against excitotoxicity. *Science* 302(5642):84–88.
4. Bellocchio L, et al. (2010) Bimodal control of stimulated food intake by the endocannabinoid system. *Nat Neurosci* 13(3):281–283.
5. Ledberg A, Robbe D (2011) Locomotion-related oscillatory body movements at 6-12 Hz modulate the hippocampal theta rhythm. *PLoS ONE* 6(11):e27575.
6. Ryan LJ (1984) Characterization of cortical spindles in DBA/2 and C57BL/6 inbred mice. *Brain Res Bull* 13(4):549–558.
7. Sirota A, et al. (2008) Entrainment of neocortical neurons and gamma oscillations by the hippocampal theta rhythm. *Neuron* 60(4):683–697.

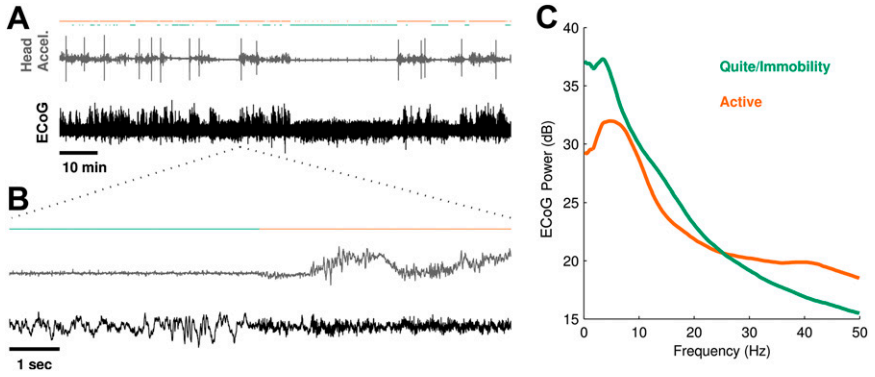

Fig. S1. Separation of immobility from mobility periods. (*A* and *B*) Illustrative experiment during which ECoG (black) and vertical head acceleration (gray) were recorded simultaneously. Orange and green lines show detected periods of activity and immobility, respectively. (*A*) Full recording; (B) 10-s epoch taken from *A*, at the time indicated by the dash lines. (*C*) Power spectrum density function of the ECoG during immobility and activity (same color code as in *A* and *B*). Note that the strong increase in ECoG power above 30 Hz during behavioral activity is partially accounted by contamination (via passive volume conduction) of the ECoG with electromyographic signals (mainly showing artifacts).

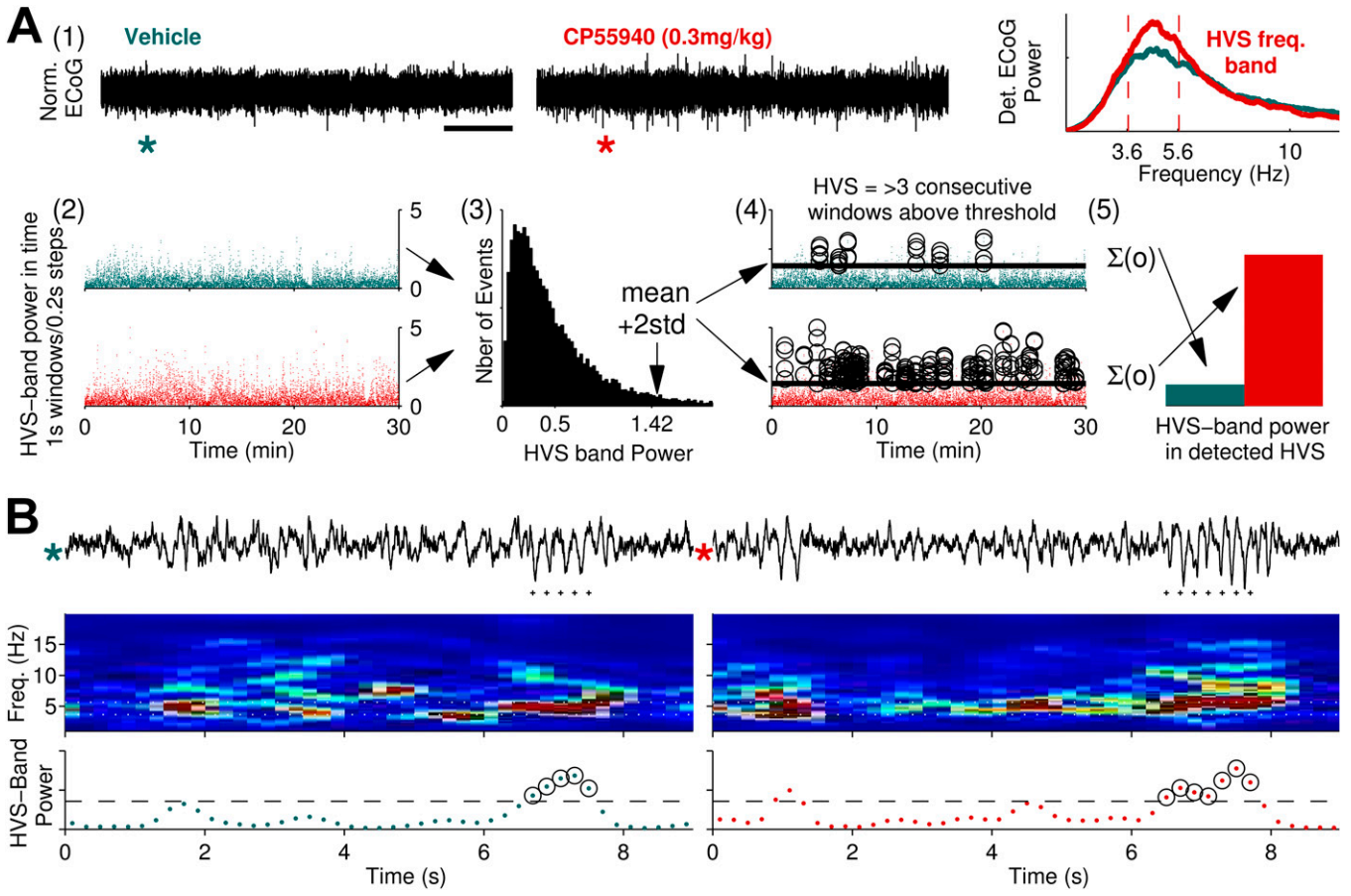

Fig. S2. Method to compare the incidence and power of HVS after vehicle and CP55940 injections. (*A*, *1*) Same-length ECoGs, recorded during immobility epochs, are compared after systemic injections of vehicle and CP55940. Power spectra of the detrended ECoGs are computed, and HVS frequency band is determined. (*A*, *2*) Time-frequency spectrograms are computed from the standardized ECoG, and the time-varying power in the HVS frequency band is reported. (*A*, *3*) Threshold detection is set as the mean plus 2 SDs of all the HVS band power values (vehicle + CP55940). (*A*, *4*) HVS are defined as at least four consecutive windows with power values above threshold. (*A*, *5*) The sum of the ECoG power (in the HVS band) from the windows detected as part of an HVS is computed for each pharmacological condition and compared. (*B*) Examples of detected HVS. (*Top*) Traces are ECoG epochs taken from *A*, at times indicated by stars. (*Middle*) Time–frequency spectrograms. White dotted lines show HVS frequency band for this experiment. (*Bottom*) ECoG power in the HVS frequency band. Dashed lines represent the threshold and circled points the values detected as part of a HVS.

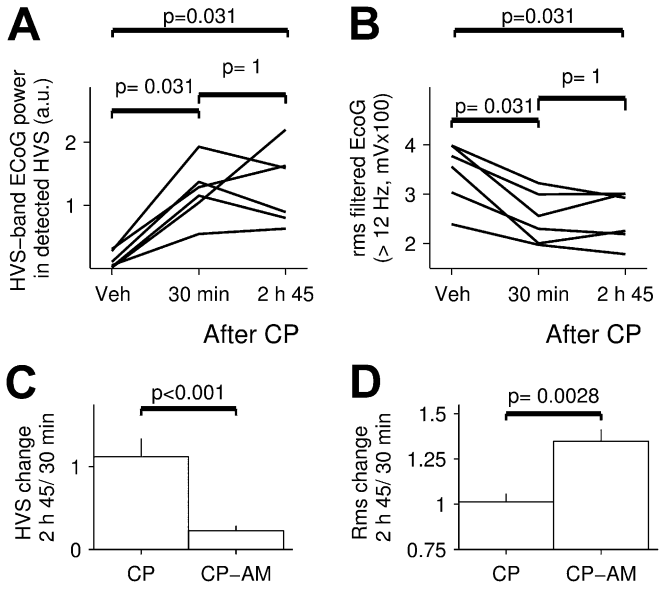

Fig. S3. CP55940 effects on HVS and fast ECoG oscillations are still present 2 h 45 min after injection and are reversed by injection of a CB1 antagonist. (*A*) HVS were compared in 30-min-long epochs (during immobility) starting 15 min after vehicle and both 15 min and 2 h 30 min after CP55940 injections (0.3 mg/kg, n = 6 experiments in six mice). (*B*) Same experiments as in *A*, but the amplitudes of fast ECoG oscillations (>12 Hz) were compared. *P* values in *A* and *B* are from Wilcoxon paired two-sided signed rank test. (*C*) Average ratio between late and immediate effects of CP55940 on HVS. Comparison is made between experiments in which only CP55940 was injected (left bar, same data as in *A*) and experiments in which an i.p. injection of AM251 was made 1 h after CP55940 injection (right bar, same data as in Fig. 1*D*). In both conditions late effects were quantified starting 2 h 30 min after the CP55940 injection. *P* value is from the Wilcoxon ranksum test. (*D*) Similar comparison as in *C*, but for the amplitude of fast (>12 Hz) ECoG oscillations. Left bar is calculated from from data in *B*, whereas right bar is from the same data as in Fig. 1*F*.

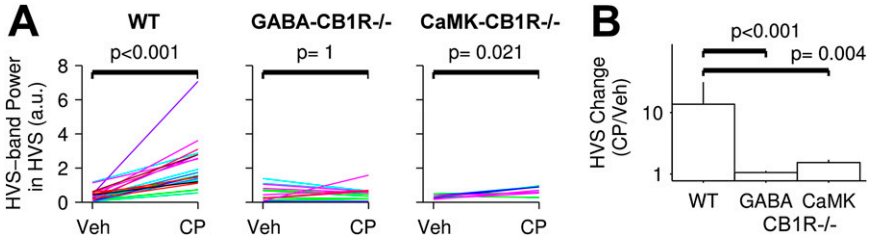

Fig. S4. Effect of CP55940 on HVS is abolished in mice lacking CB1R expression in forebrain GABAergic neurons (GABA-CB1R$^{-/-}$) and forebrain principal neurons (CaMK-CB1R$^{-/-}$). (*A*) HVS comparison in all experiments. Each line represents a single experiment, and different colors represent different animals. CP55940 (0.3 mg/kg) reliably increases HVS in WT animals. Such effect is absent in GABA-CB1R$^{-/-}$ mice and small in CaMK-CB1R$^{-/-}$ mice. *P* values are from Wilcoxon paired two-sided signed rank test. (*B*) Mean HVS change (CP55940/vehicle) + SEM for all experiments. *P* values are from Wilcoxon rank sum test vs. WT data. Note that in GABA-CB1R$^{-/-}$ and CaMK-CB1R$^{-/-}$ mice, CB1R expression is absent from D1-positive striatonigral neurons.

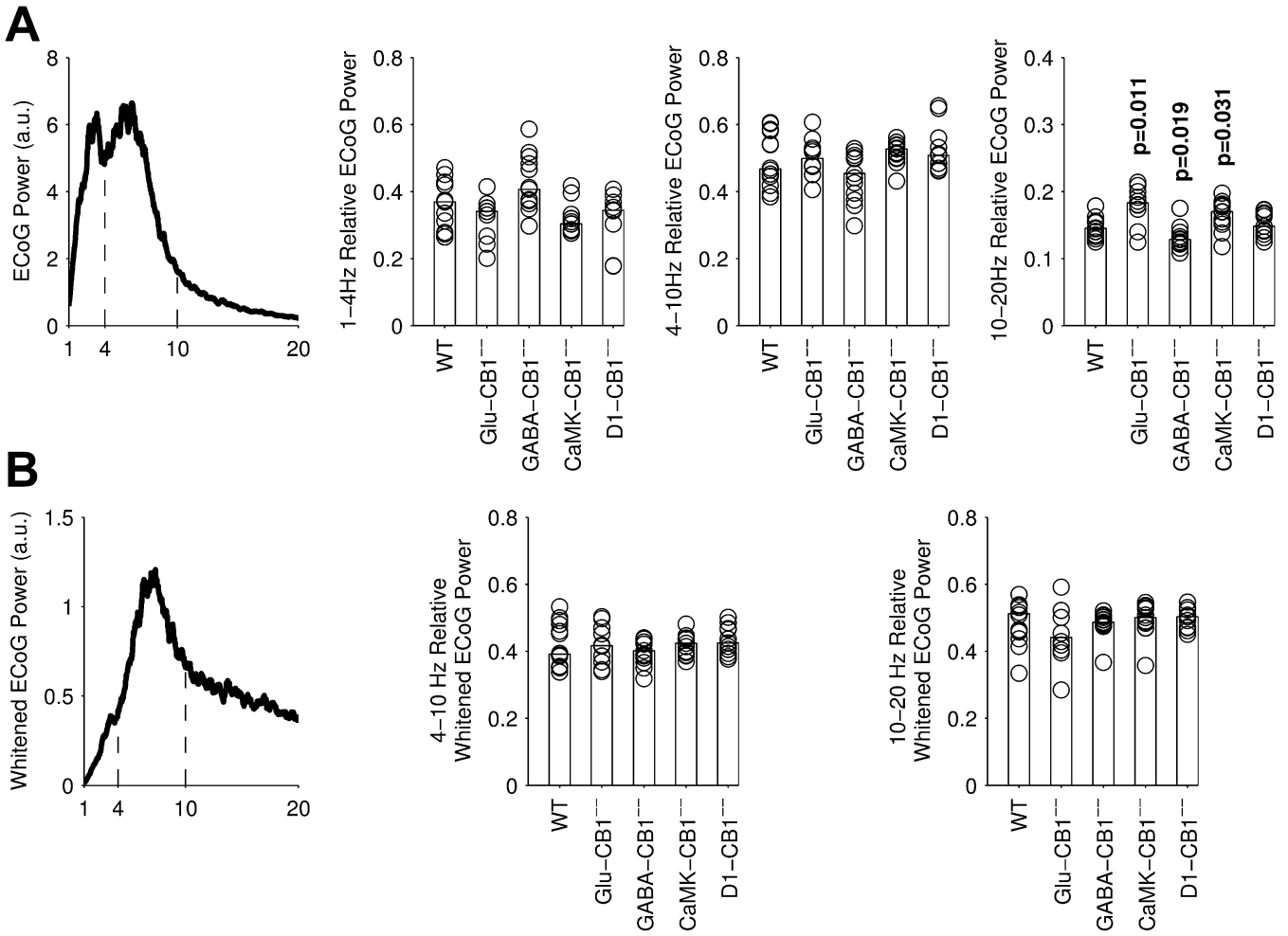

Fig. S5. Relative ECoG oscillatory content in control condition recorded from WT and CB1R conditional mutant mice. (*A*, *Left*) ECoG power spectrum density function of a representative WT mouse, in control condition. Three frequency bands (1–4, 4–10, 10–20 Hz) were arbitrarily defined. ECoG was high-pass filtered above 1 Hz. The three histograms show the ECoG relative power in the three bands during baseline or vehicle recordings for all experiments displayed in Figs. 2, 4, 5, and Fig. S4. *P* values are from Wilcoxon rank sum test vs. WT and were not graphically reported if above 0.05. (*B*) Same data as in *A*, except that the 1/f power relationship was removed from the ECoG (7). In this case, the relative power in the lowest frequency band is meaningless and is not shown. Note that there was no significant difference between WT and CB1 conditional mutant mice in the 10- to 20-Hz band.